An analysis of polarization: Ground-based upward looking and aircraft/satellite-based downward looking measurements.

Brian Cairns[a], Larry D. Travis[a] and Edgar E. Russell[b]

[a] NASA Goddard Institute for Space Studies, 2880 Broadway, New York, NY 10025
[b] SpecTIR Corporation, Goleta, CA

ABSTRACT

It is shown that it is possible to retrieve aerosol properties using polarization measurements from satellite, or aircraft even when the surface polarization is significant and unknown. This extends the domain for which it is possible to intercompare ground and aircraft/satellite estimates of aerosol properties and allows the retrieval of aerosol properties to be made above bare soil surfaces.

Keywords: Surface properties, atmospheric correction, polarization, aerosols

1. INTRODUCTION

Evidence that tropospheric aerosols can cause a direct radiative forcing comparable in magnitude, though opposite in sign, to the expected climate forcing by greenhouse gases[1,2] makes a compelling case for improved efforts to obtain accurate information about the distribution of tropospheric aerosols and their radiative impact[3]. The only method by which we would expect to obtain a global picture of the magnitude and variability of aerosol properties is from satellite measurements. As discussed by Wang and Gordon[4], the retrieval of aerosol optical thickness using satellite reflectance measurements requires an aerosol model, namely the specification of the aerosol scattering phase function and single-scattering albedo. Most often the scattering properties are modeled using Mie theory, which is valid only for spherical particle shape, because shape information is unavailable. However, as shown by Mishchenko *et al.*[5] even moderate nonsphericity results in substantial errors in the retrieved aerosol optical thickness if the data are analyzed using Mie theory. Further, even for spherical particles, it is essential to determine whether the aerosols are absorbing (e.g., biomass burning) or not (e.g., sulfate) to correctly determine the aerosol forcing. Moreover, as we discuss below erroneous assumptions about shape can lead to significant errors in the inference of absorption.

The only current remote sensing method that can retrieve both a plausible particle size distribution, surface albedo and an average complex refractive index is the combined measurement of the solar direct beam and the diffuse sky radiance[4,6,7]. This type of measurement is made on a routine basis by a worldwide network (AERONET) of instruments[8]. There are however problems with these retrievals in that uncertainty in the calibration of the sky radiometer used for these measurements can cause serious biases. By contrast polarization is a relative measurement and so the accuracy with which it can be measured is limited only by the care with which the instrument used in its measurement is designed and characterized. Indeed there are a significant number of instruments in the AERONET network that measure polarized sky radiances, though detailed analyses have only been attempted recently[9].

The difference in the quality of information available from intensity and polarization measurements is illustrated in a simple way in Figure 1. To construct this figure we calculated the distribution of intensity and polarization for an almucantar scan with a solar elevation of 30° and measurements made every 5° in azimuth, for a series of models. The calculations are made for a wavelength of 870 nm with the appropriate Rayleigh optical depth of 0.015 above the aerosol layer and a Lambertian surface below it. This wavelength was chosen since it is used for the operational AERONET network. We assumed an aerosol size distribution given by the gamma distribution[10] with an effective variance of 0.1. The base conditions for the aerosol layer are an optical depth at 550nm of 0.1, an effective radius of 0.4 μm, a refractive index of $1.45+0.0i$ and a surface albedo of 0.1. We then allowed different pairs of parameters to vary simultaneously. The vertical and horizontal lines show the location of a "true" model which we are trying to retrieve. The contours around the intersection of these dashed lines show the domains for which the "true" model is indistinguishable from other models and therefore represents the uncertainty in the retrieval. Two contours are shown on each figure. The solid line contour is drawn assuming that the expected RMS deviation of the measured polarization from the actual polarization is 0.2%. The dashed line contour is drawn assuming that

the expected RMS deviation of measured intensity from actual intensity is 4.0%. It is apparent that a reasonable retrieval of size and optical depth is obtained from intensity only measurements, provided the complex refractive index and surface albedo are well constrained *a priori*. This is in agreement with the results of Nakajima *et al.*[7] who found that the inference of optical depth from sky radiance measurements was less susceptible to calibration errors than the inference of optical depth from direct beam measurements. When we examine the simultaneous retrieval of real and imaginary parts of the refractive index and the surface albedo from a full almucantar scan we see that large errors in the inference can be made if only intensity measurements are used. These parameters can, however, be retrieved if accurate polarization measurements are made. Our choice of contour levels is based on the expected uncertainty in a single polarization measurement ~0.2% and the expected uncertainty in the calibration of radiometric measurements ~4%[8].

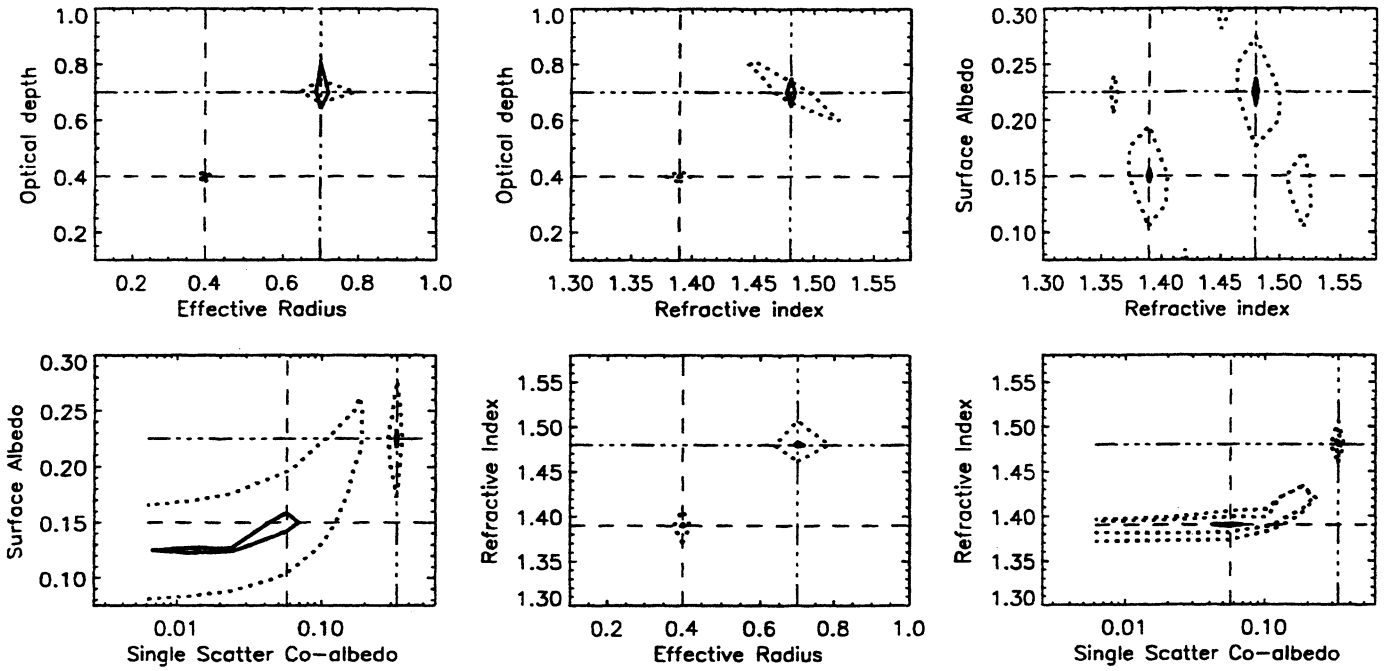

Figure 1. Showing the domains of plausible retrievals for an almucantar scan using intensity with a calibration uncertainty of 4% (dashed lines) and polarization with an uncertainty of 0.2% (solid lines), for a range of different aerosol microphysical properties.

A similar analysis can be performed for a satellite, or aircraft based instrument, looking down on an aerosol layer and is shown in Figure 2. This figure uses the intensity and polarization calculated for an instrument above the atmosphere scanning +/-60° from nadir in the plane of the sun, making measurements every 5°, with a solar elevation of 30° for a series of different aerosol models. This geometry was chosen for illustrative purposes, so that the range of scattering angles observed is the same as for the error analysis of almucantar scans shown in Figure 1. The calculations are made for a wavelength of 470 nm with a Rayleigh optical depth of 0.185. This wavelength was chosen since it is one of the wavelengths available on the RSP (see section 2) and will be used by MODIS[11] for remote sensing of aerosols over vegetated surfaces. It is also indicative of the behavior we would expect for a wavelength of 440nm, which will be used by MISR[12] and POLDER[13] for remote sensing of aerosols. The vertical structure of the atmosphere is an aerosol layer, with 50% of the molecular scattering mixed into it, above a Lambertian surface with the remaining 50% of the molecular scattering in a layer above the aerosol/molecular layer. Once again a size distribution given by the gamma distribution[10] with an effective variance of 0.2 is used. The base conditions for the aerosol layer are an optical depth at 550nm of 0.5, an effective radius of 0.4 μm, a refractive index of $1.45+0.0i$ and a surface albedo of 0.1. We then allowed different pairs of parameters to vary simultaneously. The contours shown have the same meaning as in Figure 1. Note that each row of figures in Figure 2 can be regarded as a front, side and top section of the three dimensional domain of retrieved parameters that are consistent with the accuracy of the measurements. The first row of Figure 2 demonstrates the well known fact that the retrieval of aerosol optical depth and effective radius above a bright surface using intensity measurements only is extremely uncertain, although using multiple angle intensity measurements[12] above a dark surface it is possible to retrieve optical depth and effective radius

with a good degree of accuracy, provided the single scatter albedo of the aerosol layer is known. It is also apparent that using intensity only measurements, of a single scene, at a single wavelength, it is not possible to unambiguously retrieve both the surface albedo and an aerosol single-scatter albedo. These parameters can, however, be retrieved if accurate polarization measurements are made.

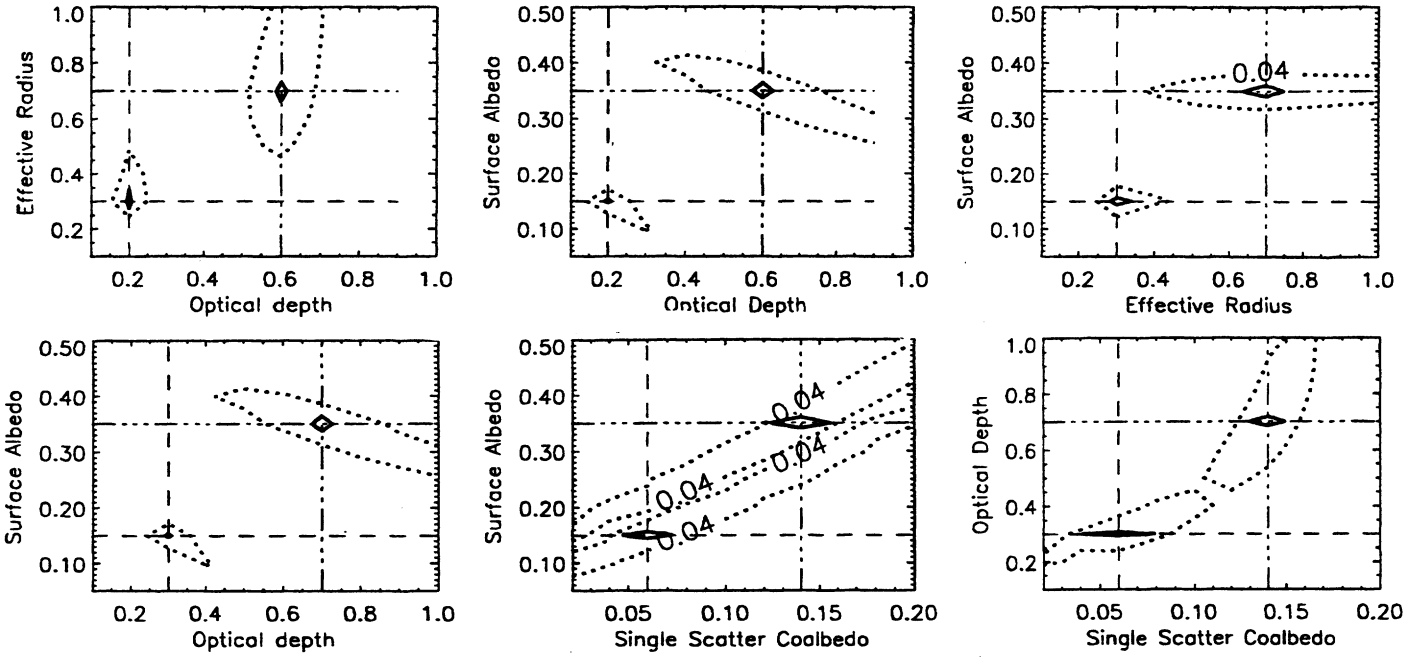

Figure 2. Showing the domains of plausible retrievals for a zenith scan using intensity with a calibration uncertainty of 4% (dashed lines) and polarization with an uncertainty of 0.2% (solid lines), for a range of different aerosol microphysical properties.

In order to effectively deal with atmospheric aerosols it is also necessary to be able to recognize the presence of nonspherical particles. This is because the phase function of a non-spherical particle can be mimicked by increasing the real and imaginary parts of the refractive index of a spherical particle of the same surface equivalent size[14]. Figure 3a shows two elements of the phase matrix for a shape mixture of nonspherical particles[15] (solid line) and a polydispersion of spheres (dashed line) with the same size distribution and a refractive index of 1.53+0.0055*i* at a wavelength of 550nm. Figure 3b shows two elements of the phase matrix for a shape mixture of nonspherical particles (solid line) and a polydispersion of spheres (dashed line)

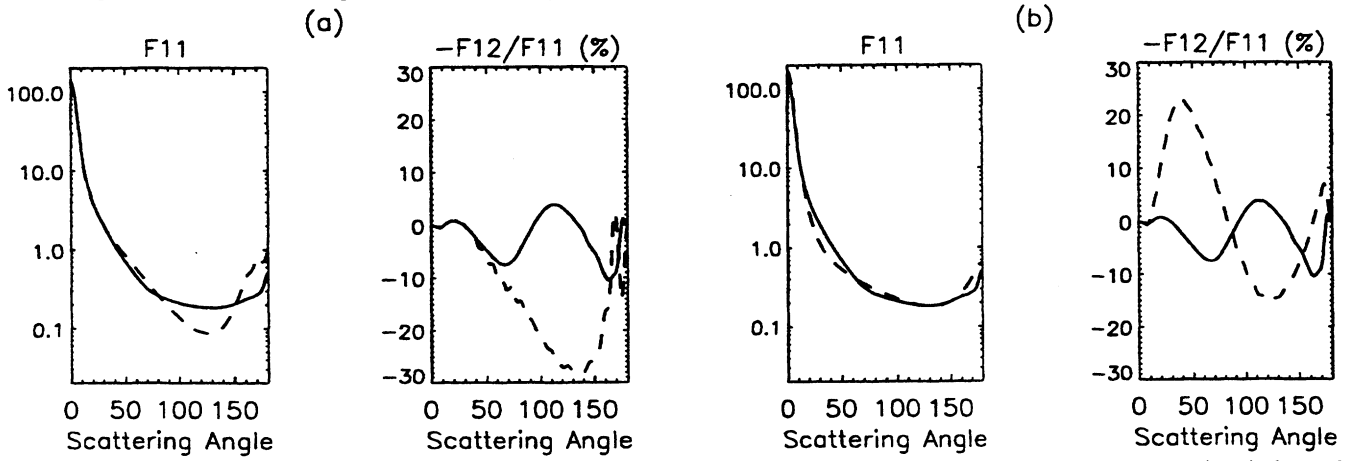

Figure 3a) Phase matrix elements for a shape and size mixture of nonspherical particles with a refractive index of 1.53+0.0055*i* (solid line) and for a surface equivalent size distribution of spheres with the same refractive index (dashed line).

3b) Same as a) except that the refractive index is 2.25+0.025*i* for the surface equivalent size distribution of spheres.

with the same size distribution and a refractive index of 2.25+0.025*i* at a wavelength of 550nm. The phase function behavior of the nonspherical particles is obviously well approximated by the polydispersion of spheres with a refractive index of 2.25+0.025*i*. However, the polarization properties (-F12/F11) are not well modelled by spheres with a spuriously large refractive index and the single-scatter coalbedo is overestimated by a factor of three. The inability to simultaneously match intensity and polarization measurements of non-spherical particles with surface equivalent spheres suggests that it should be possible to differentiate between non-spherical and absorbing particles, using polarimetric measurements[13].

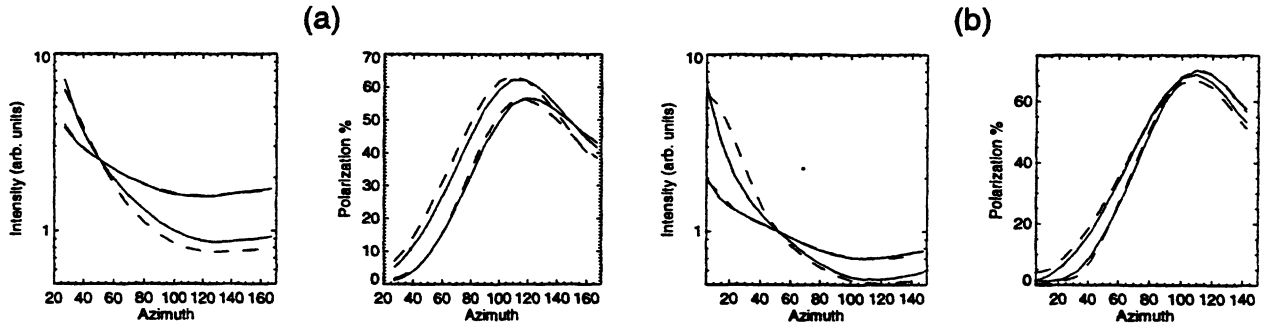

Figure 4. Intensity and polarization of downwelling skylight at 410nm and 678nm (solid line) and theoretical fit based on a table look up of aerosol models (dashed line).

Figures 1 and 2 demonstrate that the aerosol properties retrieved using polarized radiance measurements should be sufficiently robust and accurate to allow for a meaningful intercomparison between aircraft/satellite and ground-based measurements. The ability to estimate surface albedo and aerosol properties from both aircraft/satellite and ground-based measurements suggests that it should be possible to bootstrap the aerosol retrievals by using both sets of measurements together. In Figure 4 we present some polarized sky radiance measurements that can be used to examine whether a parametric estimation of aerosol properties similar to that presented in Figures 1 and 2 is adequate for real aerosol measurements. These measurements were obtained using the Galileo PhotoPolarimeter Radiometer[16] (PPR) engineering spare modified to make it suitable for the acquisition of sky radiance and polarization data. The data shown in Figure 4 were acquired in Goleta CA. The figures show the data (solid lines) and the model fit (dashed lines) at 410nm and 678nm. The assumed aerosol size distribution used is a single mode gamma distribution[10] with an effective variance of 0.1 and the single scatter albedo was assumed to be unity. A database of 625 multiple scattering calculations was then generated as a function of real refractive index, effective radius, surface albedo and optical depth at both wavelengths and an overall best fit for both intensity and polarization at 410nm and 678nm was found. The data in Fig. 4a was obtained on 4th April 1996 and has a best fit for an effective radius of 0.3μm, a refractive index of 1.5 an optical depth (@550nm) of 0.06 and a surface albedo of 0.1. The data in Fig. 4b was obtained on 21st October 1996 and has a best fit for an effective radius of 0.5μm, a refractive index of 1.4 an optical depth (@550nm) of 0.02 and a surface albedo of 0.15. The only correlative information available to check the results found in this analysis of polarization were surface albedo estimates made from AVHRR channels 1 and 2, which were in agreement with the inferred surface albedo. The inclusion in the data base of the effective variance and imaginary part of the refractive index would allow us to obtain a better fit between the data and the model, as would an iterative scheme which estimates the size distribution[4,7,17]. However the absence of correlative data from sunphotometry, or sky radiometers that accurately measure the solar aureole, limits our ability to compare the retrievals of aerosol properties from these polarization measurements with retrievals using currently accepted methods. The collection of more data at a well instrumented site in the coming months will eliminate this problem and allow for a more detailed analysis of the retrieval process.

It is apparent from Figure 4 that much of the variability in the data can be represented by the variation of optical depth, surface albedo and refractive index and that the effects of a size distribution on the polarized radiances are well repesented by the effective radius and effective variance of the distribution[10]. On this basis it would appear straightforward to compare

ground-based measurements with aircraft, or satellite measurements of polarization. The only difficulty is the different effect of the surface on the two measurements. For upward looking measurements the surface has a relatively weak effect on the downwelling polarized radiances and one which is insensitive to the details of the surface bidirectional reflectance and polarization properties[9]. Conversely the upwelling polarized radiances observed by a an aircraft, or satellite borne polarimeter are more strongly affected by the surface bidirectional and polarization properties. Over vegetation for which the polarized reflectance is relatively small[18,19] we expect to use polarization measurements in the blue or near UV for the comparison of upward and downward looking measurements. This is because there is a relatively weak contribution from the surface to the upwelling polarized radiance at these wavelengths compared with the strong contributions of Rayleigh scattering and aerosol scattering. The comparison of upward looking and downward looking measurements and the retrieval of aerosol properties over bare soils is somewhat harder since, as shown in Figure 5, the polarized reflectance of soil for typical viewing conditions can be quite high. In the next section we briefly describe the instruments that we will be using to make polarization measurements and in the following section suggest a method by which the surface polarization can be estimated and its effect on the retrieval of aerosol properties reduced. Simulations of the algorithm are presented in section 4 and some conclusions about the success and potential problems with the method are given in section 5.

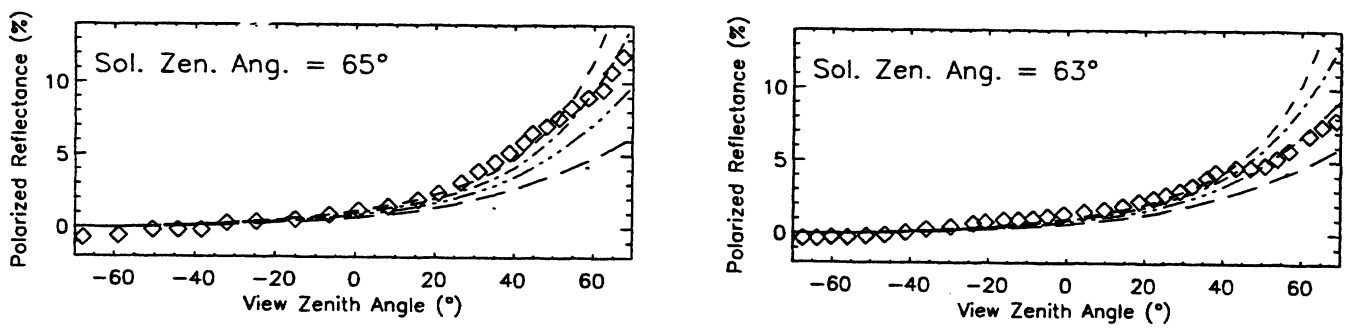

Figure 5, Polarization of soil surfaces, square symbols, adapted from measurements made by Breon *et al.*[20]. Model fits are shown by lines, see Section 3.2 for details.

2. INSTRUMENTATION

An "engineering spare" of the Galileo Photopolarimeter/Radiometer (PPR) measures the state of polarization to within 0.1% for wavelengths of 410, 678 and 945 nm. The sky radiance measurements although lacking an accurate absolute calibration nonetheless provide useful information about the microphysical properties of aerosols since the response of the instrument is linear to better than 1% over its entire dynamic range. The instantaneous field of view of this instrument is 0.14° provided by a Cassegrain Dall-Kirkham telescope. A Wollaston prism is used to produce two spatially separated orthogonal polarization states which are measured simultaneously. Half wave retarders are positioned to produce χ+0°, χ+45° and χ+90° in successive measurements. The first two retarder positions allow the degree and plane of polarization to be evaluated while the third measurement provides a check on scene stability and detector gain by interchanging the roles of the two detectors as compared to the first retarder position. The measurements are acquired using a laptop PC and each measurement cycle of 23 seconds is time stamped so that the movement of the sun during the course of data acquisition can be included in model calculations.

The Research Scanning Polarimeter (RSP) will make polarization measurements in nine spectral bands. In the visible/near infrared (VNIR) blue enhanced silicon photodiodes will be used to make measurements in six spectral bands at 410nm, 470nm, 555nm, 670nm, 865nm and 960nm. In the short wave infrared (SWIR) HgCdTe detectors cooled to selectable temperatures between 140K and 180K will be used to make measurements in three spectral bands at 1590nm, 1880nm and 2250nm. The optical system consists of six boresighted refractive telescopes. Each telescope is used for three spectral bands and two orthogonal polarization states which are spatially separated using a Wollaston prism. Telescopes that measure the

same three spectral bands are paired so that the orientation of the polarization measurement in one is rotated 45° with respect to the other. This means that the Stokes parameters Q and U are measured simultaneously[10], Q in one telescope and U in the other. By putting the SWIR spectral bands in one pair of telescopes and the VNIR spectral bands in the other two pairs good field of view matching between the telescopes can be obtained and the achromatic design of the refractive telescopes is simplified. The instantaneous field of view (14mrad) of each telescope is scanned through an angle of 120 degrees using a polarization-insensitive system. This system consists of two mirrors each used at 45° angle of incidence and with their planes of incidence oriented orthogonally to each other. During the course of a scan 152 samples are taken plus ten dark samples with a sample dwell time of 1.875msec. The instrument is designed to make either ground-based or aircraft-based measurements with a polarimetric accuracy of better than 0.2%.

3. RETRIEVAL METHOD

3.1 VECTOR DOUBLING/ADDING CODE

In order to make good use of such accurate polarization measurements a similarly accurate simulation of polarization created by various aerosol models embedded in a molecular atmosphere is required. The modified vector doubling/adding code[10] that we have developed is fast, accurate and minimizes storage requirements. The algorithm used is essentially the same as that presented by Hansen and Travis[10] and the modifications, which improve speed and accuracy are based on the work of de Haan *et al.*[21]. Like most multiple scattering algorithms, a Fourier decomposition in azimuth is used to simplify the calculation since successive Fourier components are independent of one another and the decomposition usually reduces the computational burden and storage requirements[21]. One problem with the Fourier decomposition in azimuth of the radiance field is that when large particles are present it may require a large number of Fourier terms to accurately describe the radiation field. This problem is mitigated by the observation that multiple scattering tends to wash out sharp scattering features. Thus we would expect the high frequency, high index, Fourier terms in the expansion of the radiance field to be dominated by low order scattering, ie. first and second order scattering events. The Fourier decomposed single scattering contribution is therefore subtracted out of each Fourier term in the decomposition of the radiance field. It can then be added back in exactly when it is required to calculate the radiance at a particular observation point. The Fourier decomposition can therefore be terminated when the radiance field is well approximated by single scattering at some Fourier index which we will denote M_1. Although for Fourier indices lower than M_1 the radiance is not sufficiently accurately modelled using a single scattering approximation the Fourier terms with index lower than M_1 will be well approximated by a second order scattering approximation down to some Fourier index M_2 at which point a full doubling calculation is required to accurately evaluate the radiance. Thus the calculation is broken up into three stages. A doubling calculation for Fourier indices from zero to M_2, a second order calculation from M_2 to M_1 and then exact evaluation of the single scatter contribution for actual observation points. The speed of the calculation is determined by M_2 since the slowest part of the calculation is the doubling, while the storage requirements are determined by M_1 since it is at this index that the Fourier decomposition is terminated. These two parameters can be determined, based on the required accuracy, as part of the multiple scattering calculation, since this presents a negligible computational burden.

The model atmosphere that is used in the following calculations is a two layer atmosphere with a pure molecular layer containing half the Rayleigh optical depth above an aerosol layer mixed with the other half of the Rayleigh scattering above a Lambertian surface. This vertical distribution of scattering properties is reasonable if most of the aerosol is contained in the bottom 2-3km of the atmosphere. This model can be easily modified to include different vertical profiles and over weakly polarizing surfaces such as vegetation it should be possible using polarization measurements at 410nm and 470nm to estimate the height of the aerosol layer. The downwelling radiation at the surface and the upwelling radiation at any height can be calculated following de Haan *et al.*[21] In what follows we analyze the reflected radiances at the top of the atmosphere, since provided an aircraft is above the majority of the aerosol layer there is little qualitative difference between simulated aircraft and satellite measurements.

3.2 SURFACE MODEL

In Figure 5 we have shown the measurements[20] as boxes and overlayed lines representing four theoretical model curves. The model suggested by Breon *et al.*[20] assumes that the polarized reflectance of the surface is caused by Fresnel reflection from isotropically distributed facets. The polarized reflectance for such a model has the simple form,

$$R_P^{Surf}(\mu,\mu_0,\varphi)=\frac{F_P(\mu,\mu_0,\varphi)}{4\mu\mu_0} \tag{1}$$

where F_p is simply the polarized Fresnel reflection coefficient for the given viewing geometry. The polarized reflection coefficient is uniquely determined by the viewing geometry and the refractive index of the facets[22]. μ and μ_0 are the cosine of satellite zenith viewing angle, θ, and solar zenith angle, θ_0, respectively and φ is the azimuth of the satellite viewing direction with respect to the sun. The short dashed line in Figure 5 is given by the model eq.(1) with a refractive index of 1.5. This model provides a good fit over most view angles and the refractive index is consistent with measured refractive indices of rocks and glasses, suggesting the assumptions made in this model are reasonable.

As noted by Breon *et al.*[20] this formulation is not satisfactory for limb viewing, or illumination, since mutual shadowing of facets is neglected. This omission can easily be remedied using a simple formulation of shadowing developed to explain the ocean horizon[23]. The reflectance is simply modified by a shading factor for the viewing and illumination angles. The shading factor based on a Gaussian distribution of surface slopes is given by the expression

$$S(\theta)=\frac{2}{1+erf(\nu)+(\nu\sqrt{\pi})^{-1}\exp(-\nu^2)} \tag{2}$$

where

$$\nu=\sigma\sqrt{2}^{-1}\cot(\theta) \tag{3}$$

and σ^2 is the mean square slope of the surface; ie. the larger σ^2 the rougher the surface. With the inclusion of these shading factors the polarized reflectance does not diverge even for limb viewing, or limb illumination, provided the surface has some roughness ($\sigma^2 > 0$). The remaining model curves in Figure 5 use the shading function given by eq.(2), applied to both the viewing and illumination angles for the polarized reflectance given by eq.(1) with a refractive index of 1.5. It appears that a good fit to the measurements in Figure 5a is obtained for a model in which the mean square slope is 0.25, while the measurements in Figure 5b are best fitted by a model for which the mean square slope is 0.5. The apparently greater roughness of the surface from which the measurements in Figure 5b were obtained compared with the surface from which the measurements in Figure 5a were obtained is consistent with the observed apparent roughness of the two surfaces ref.

3.3 RETRIEVAL METHOD

We now have a model of the surface that has no pathological behavior and that matches observed polarization properties of soil surfaces reasonably well. The problem is now how to remove the influence of the surface from the observed polarized radiances at the top of the atmosphere. The observed polarized radiances are given by the following expression

$$R_P^{Obs}(\lambda)\approx T(\lambda)R_P^{Surf}(\lambda)+R_P^{Atm}(\lambda) \tag{4}$$

where we are neglecting multiple reflections between surface and atmosphere and R_P^{Atm} is the polarized radiance for an atmosphere above a nonpolarizing, or Lambertian, surface

$$T(\lambda)=\exp[-\tau_\lambda(1/\mu+1/\mu_0)] \tag{5}$$

and τ_λ is the total optical depth at a wavelength λ. In practice the use of the transmission of the direct beam given by eq.(5) understimates the effective transmission of polarized relectance from the surface to the top of the atmosphere and we found it more effective to use a reduced optical depth, $\tau_{r\lambda}$, corrected for forward scattering of the aerosols, viz., $\tau_{r\lambda}=\tau_\lambda(1-g)$ where g is the asymmetry parameter. Although this optical depth is probably reduced too much[20] we will see in section 4 that our initial estimates of optical depth tend to be too large so these errors tend to compensate one another. We note that the

observed polarized reflectance of soil surfaces[20] and measurements of rock and glass refractive indices[24] show negligible variation with wavelength over a very wide spectral range. Thus we might expect that the use of spectral differences could help to eliminate the contribution of surface polarization since the spectral differences in polarized radiances should be dominated by spectral differences in molecular scattering and aerosol properties. We write the spectral difference of the observed polarized radiances as

$$\Delta R_P^{Obs}(\lambda_1,\lambda_2) \approx \Delta T(\lambda_1,\lambda_2) R_P^{Surf} + \Delta R_P^{Atm}(\lambda_1,\lambda_2) \tag{6}$$

where the operator Δ is defined to be

$$\Delta X(\lambda_1,\lambda_2) = X(\lambda_1) - X(\lambda_2) \tag{7}$$

If the surface polarization multiplied by the spectral difference in transmissivity $\Delta T(\lambda_1,\lambda_2) R_P^{Surf}$ is small compared with the spectral difference in polarized radiances caused purely by aerosol/molecular scattering $\Delta R_P^{Atm}(\lambda_1,\lambda_2)$ we can estimate aerosol radiative properties such as optical depth and effective radius. This is done using a look-up table of calculations of $\Delta R_P^{Atm}(\lambda_1,\lambda_2)$ for a range of aerosol sizes and optical depths. The optical depth and aerosol size are obtained from the best fit of $\Delta R_P^{Atm}(\lambda_1,\lambda_2)$ to $\Delta R_P^{Obs}(\lambda_1,\lambda_2)$. Once we have this initial, if imperfect, estimate of the aerosol radiative properties we can return to eq.(4) and estimate the surface polarization. The estimate of surface polarization is obtained from the following expression

$$R_P^{SurfEst}(\lambda) = \frac{R_P^{Obs}(\lambda) - R_P^{AtmEst}(\lambda)}{T^{Est}(\lambda)} \tag{8}$$

where $R_P^{AtmEst}(\lambda)$ and $T^{Est}(\lambda)$ are obtained from look-up tables using our initial estimates of aerosol optical depth and size. Combining the aerosol radiative properties estimated from eq.(6) and the estimate of the surface polarization given by eq.(8) we have an estimate of the surface contribution in eq.(6), that we previously neglected. By correcting the observed spectral difference in polarized radiance for the estimated surface contribution we obtain a better estimate of the spectral difference in polarization for an atmosphere above a nonpolarizing surface, which is given by the expression

$$\Delta R_P^{Atm}(\lambda_1,\lambda_2) \approx \Delta R_P^{Obs}(\lambda_1,\lambda_2) - \Delta T^{Est}(\lambda_1,\lambda_2) R_P^{SurfEst} \tag{9}$$

The best fit of look-up table calculations to this corrected spectral difference gives us a better estimate of the aerosol optical depth and size.

In principal the retrieval method embodied in eqs.(6)-(9) could be iterated, but in practice a fairly good estimate of the aerosol properties is obtained after only one application of this scheme. It is important to note that at no point is a model calculation for an atmosphere above a polarizing surface required. The estimates of aerosol properties are always made using ΔR_P^{Atm} the spectral difference for an atmosphere above a nonpolarizing surface, while the polarization of the surface is estimated from the observations.

4. SIMULATED RETRIEVALS

The retrieval method introduced in section 3.3 appears to be most useful when applied to wavelengths for which Rayleigh scattering is negligible, so that the spectral differences are dominated by the spectral variation of aerosol properties. The retrievals presented using this method are therefore simulated for wavelengths of 870, 1600 and 2250nm. We also demonstrate that aerosol properties can be retrieved at 410, 470 and 550nm in the presence of a polarizing surface by using the surface polarization estimate from the longer wavelengths.

All of the results shown in this section are for an instrument above the atmosphere scanning +/-60° from nadir, making

measurements every 5°, with a solar zenith angle of 60° and the azimuth angle from the sun being 120° on one half of the

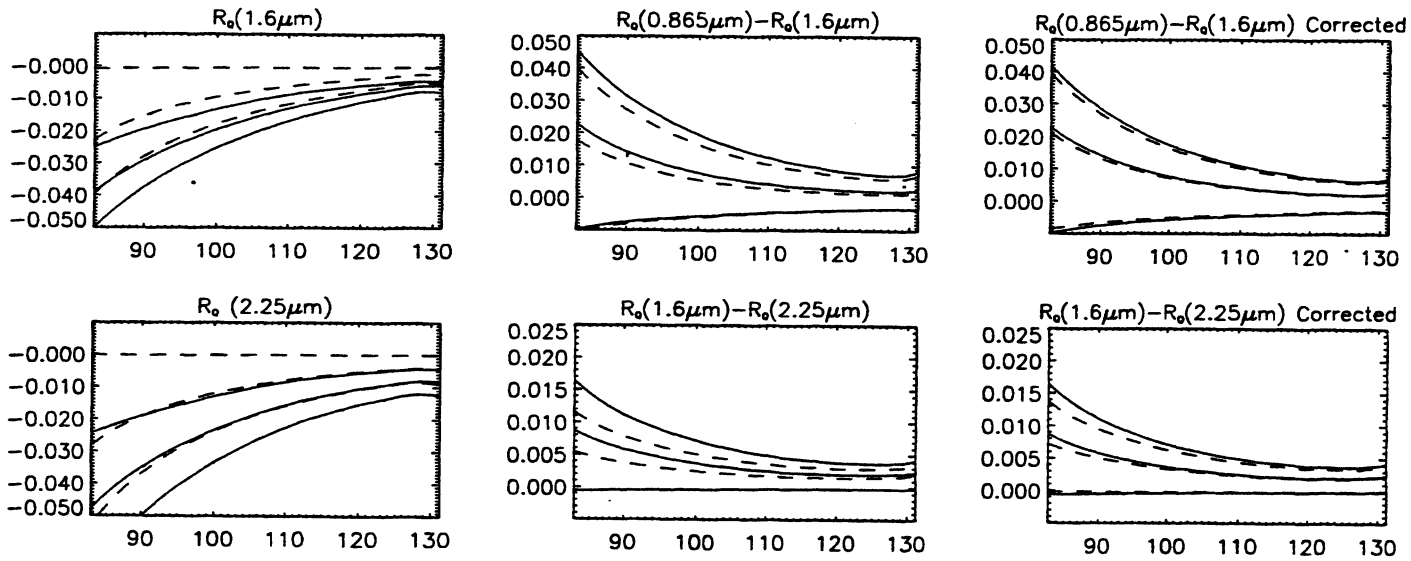

Figure 6. Polarized radiances and spectral differences of polarized radiances for "observations" of aerosols above a simulated soil surface (solid lines) and for simulations of aerosol above a Lambertian surface.

scan and -60°on the other half. In the following simulations we have used the model of polarized surface reflectance given by eq.(1) for a refractive index of 1.5, modified by the shading factors of eq.(2) with a mean square slope of 0.5 ie. comparable with measurements shown in Figure 5b. The surface albedo is assumed to be 0.1, which is too low for most soil surfaces at the wavelengths we are considering. However, since polarized radiances are scarcely affected by the magnitude of the surface albedo this is of little concern for the analysis presented here. The soil surface model is used in the doubling/adding code described in section 3.1 to create a set of "observations". We then use the method described in section 3.3 to retrieve aerosol radiative properties from the "observations" using calculations of polarized radiances at the top of the atmosphere, for an underlying Lambertian surface. In the left two plots of Figure 6 are shown the "observed" polarized radiance and the polarized radiance simulated assuming a Lambertian surface for 1600nm and 2250nm. Increasingly negative polarized radiances correspond to increasing aerosol optical depths (0.0, 0.5 and 1.0 at 550nm). Obviously using an aerosol layer above a Lambertian surface does not allow us to accurately retrieve aerosol optical depth above a polarizing soil surface. The center two plots in Figure 6 show the spectral differences for "observed" polarized radiance (solid lines) and the spectral differences for polarized radiance simulated assuming a Lambertian surface (dashed lines). Increasingly positive spectral differences correspond to increasing aerosol optical depths. We see that using spectral differences it is possible to obtain plausible estimates of aerosol optical depth, even when the underlying surface is polarizing. We also observe that estimates of optical depth made using this simple spectral difference will be too large. The right two plots in Figure 6 show the spectral differences for "observed" polarized radiance (solid lines) and the spectral differences for polarized radiance simulated assuming a Lambertian surface (dashed lines), but corrected using eq.(9). Increasingly positive spectral differences correspond to increasing aerosol optical depths. The correction given by eq.(9) moves the "observations" (solid lines) and the polarized radiances simulated using a nonpolarizing surface and the contribution of surface polarization estimated from the "observations" (dashed lines) closer together, which indicates an improved estimate of optical depth.

Figure 7 summarizes this behavior for the simultaneous retrieval optical depth and effective radius. The crossed lines indicate the location of an "observation". The solid contours indicate the domain for which spectral differences of polarized radiance calculated using a Lambertian surface are consistent with this observation, the dashed lines indicate the domain of spectral differences of intensity that are consistent with this observation. The contours are drawn assuming that an RMS error of 4% is the best that can be achieved in calibrating the instrument. The first line of plots in Figure 7 represents a retrieval of

aerosol optical depth and effective radius using spectral differences, in which no correction for the surface contribution has been made, while the second row shows how accurate the retrieval can be made by including the correction given in eq.(9). In Figure 7 the extremely good retrievals of aerosol optical depth and effective radius obtained using intensity are unrealistic. This is because it is assumed that the albedo is known exactly and has no spectral variation ie. the "observations" and simulations have exactly the same albedo. This does not affect our conclusions regarding the polarized radiances since the spectral variation of surface polarization is very weak and polarized radiances are not stongly affected by surface albedo, but means that such good retrievals using intensity are unrealistic.

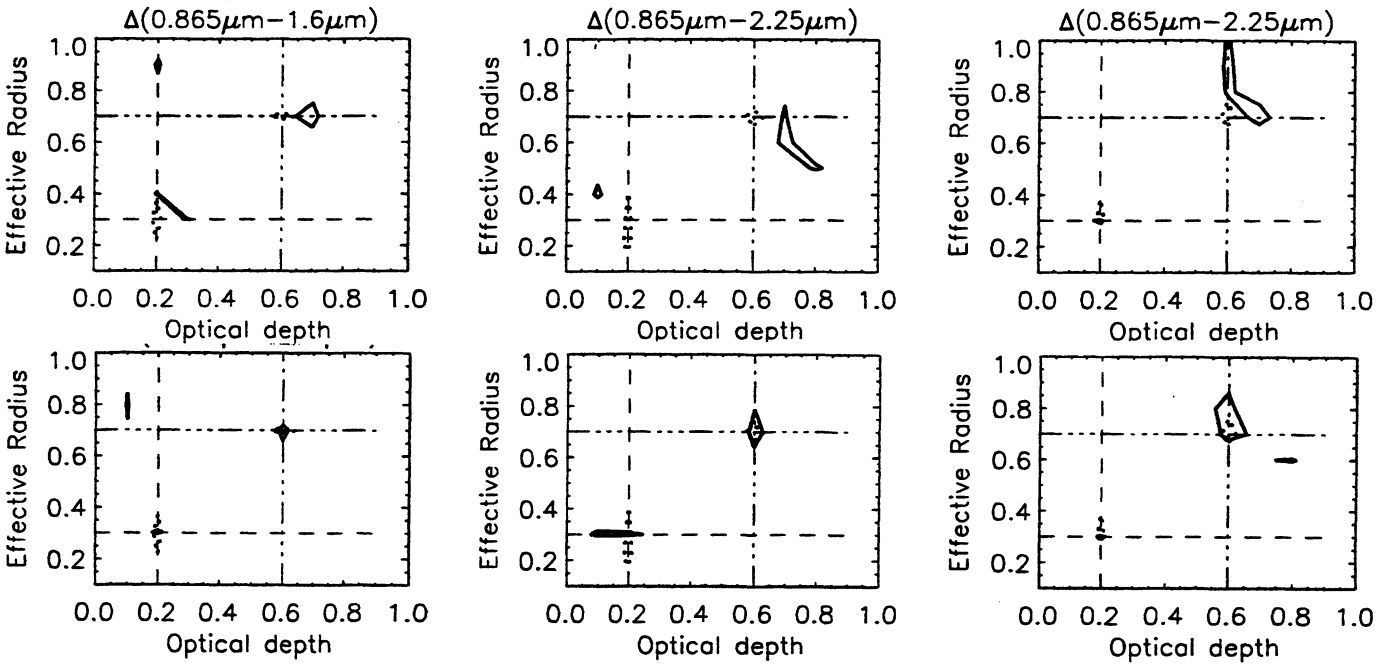

Figure 7. Showing the domains of plausible retrievals for a zenith scan using intensity with a calibration uncertainty of 4% (dashed lines) and polarized intensity with an uncertainty of 4.0% (solid lines), for a range of different aerosol microphysical properties.

Figure 8 shows the retrievals of optical depth and effective radius that can be achieved at short wavelengths using the estimate of surface polarization given by eq.(8). It should be noted that the larger the aerosol optical depth the worse the accuracy of the retrieved surface polarization. This problem is offset by the fact that aerosol optical depths, for most types of aerosol, are substantially larger at shorter wavelengths and so the contribution of the surface to the observed polarized radiance [cf. eq.(4)] is smaller for larger aerosol optical depths. The solid line contour is drawn assuming that the expected RMS deviation of the measured degree of polarization from the actual polarization is 0.2%. The dashed line contour is drawn assuming that the expected RMS deviation of measured intensity from actual intensity is 4.0%.

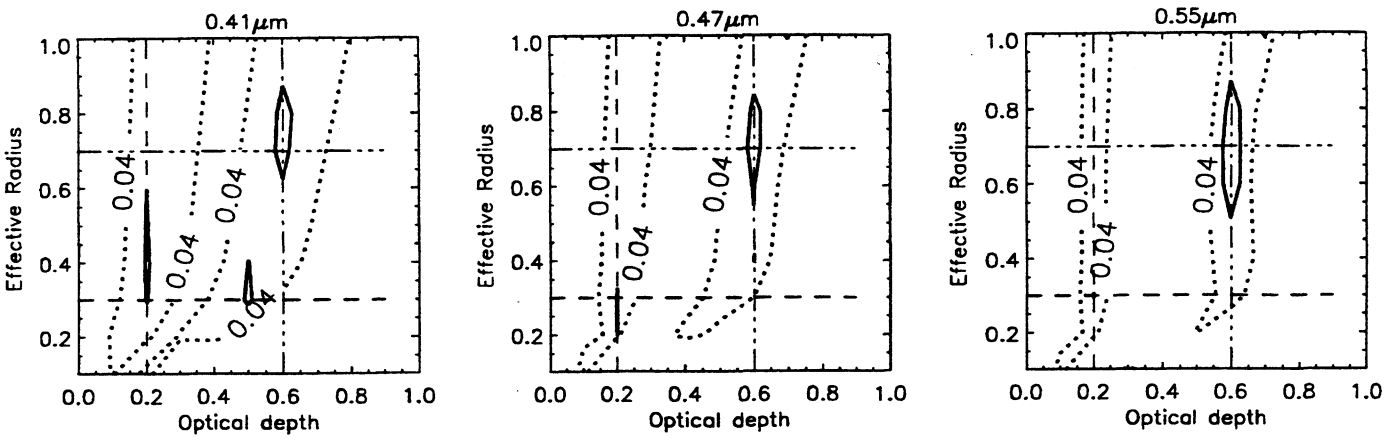

Figure 8. Showing the domains of plausible retrievals for a zenith scan above a soil surface using intensity with a calibration uncertainty of 4% (dashed lines) and degree of polarization with an uncertainty of 0.2% (solid lines).

4. CONCLUSIONS

We have shown that even when the surface polarization of a soil surface is unknown the spectral differences between channels in the near infra-red can be used to estimate aerosol radiative properties. Once the aerosol radiative properties have been retrieved it is then possible to perform atmospheric correction to obtain the surface polarized reflectance. These retrievals require that the spectral variation of surface polarization properties be weak and that a broad spectral range of measurements, where Rayleigh scattering is negligible, be available. The reason for requiring that Rayleigh scattering be negligible is because otherwise the spectral differences are dominated by molecular scattering and so small errors in the spectral difference are magnified in the estimates of aerosol properties. The requirement of a broad spectral range is so that the spectral differences in aerosol properties are sufficiently large that they can be accurately measured. Once the aerosol properties and surface polarized reflectance have been estimated in the near infra-red the reflectance properties can be used in the visible spectral range to check the aerosol retrieval. Any errors in the estimate of surface polarized reflectance, caused by spectral variation between the near infra-red and the visible, or inaccuracies in the near infra-red atmospheric correction are mitigated by the large molecular and aerosol optical depths in the visible spectral range. This is because the principal contribution of the surface to the polarization at the top of the atmosphere is from a single reflection off the surface and this is reduced by the two way atmospheric transmission from the top of the atmosphere to the surface and back.

These results demonstrate that even when the surface polarization properties are unknown the accuracy of the aerosol retrieval using polarization is very good. Indeed our results show that the accuracy of retrieved aerosol properties using polarization over a surface with an unknown polarized reflectance is comparable with the results for intensity when the surface properties are known precisely. This suggests that accurate polarization measurements may be the only means by which aerosol properties can be retrieved over a bright soil surface from space.

REFERENCES

1. Hansen, J.E., and A.A. Lacis, Sun and dust vs. greenhouse gases; an assessment of their relative roles in global climate change, *Nature*, **346**, 713-719, 1990.

2. J.E. Penner, R.J. Charlson, J.M. Hales, N.S. Laulainen, R. Leifer, T. Novakov, J. ogren, L.F. Radke, S.E. Schwartz, and L. Travis, Quantifying and minimizing uncertainty of climate forcing by anthropogenic aerosols, *BAMS*, **75**, 375-400, 1994.

3. J.E.Hansen, W. Rossow, and I. Fung, Long-Term Monitoring of Global Climate Forcings and Feedbacks, NASA Conf. Publ. 3234, NASA/GSFC 1993.

4. M. Wang and H.R. Gordon, Retrieval of the columnar aerosol phase function and single-scattering albedo from sky radiance over the ocean: simulations. *Appl. Opt.*, **32**, 4598-4609 1993.

5. M.I. Mishchenko, L.D. Travis, A.A. Lacis and B.E Carlson, Satellite remote sensing of nonspherical tropospheric particles. *Proc. SPIE*, **2311**, 150-161, 1994.

6. M. Wendisch and W. von Hoyningen-Huene, High speed version of the method of 'successive order of scattering' and its application to remote sensing. *Beitr. Phys. Atmosph.*, **64**, 89-91, 1991.
7. T. Nakajima, G. Tonna, R. Rao, P. Boi, Y.J. Kaufman, and B.N. Holben, Use of sky brightness measurements from ground for remote sensing of particulate polydispersions. *Appl. Opt.*, **35**, 2672- 2686, 1996.
8. B.N. Holben, T.F. Eck, I. Slutsker, D. Tanre., J.P. Buis, A. Setzer, E. Vermote, J.A. Reagan, Y.J Kaufman, T. Nakajima, F. Levenu, I. Jankowiak and A. Smirnov, Automatic sun and sky scanning radiometer system for network aerosol monitoring, *Remote Sens. Env.*, submitted, 1997.
9. Breon, F-M, J.L. Deuze, D. Tanre and M. Herman, Validation of spaceborne estimates of aerosol loading from Sun photometer measurements with emphasis on polarization, *J.Geophys.Res.*, **102**, 17187-17195, 1997.
10. J.E. Hansen and L.D. Travis, Light scattering in planetary atmospheres, *Space Sci. Rev.*, **16**, 527-610, 1974.
11. Kaufman Y.J. and D. Tanre, Strategy for direct and indirect methods for correcting aerosol effect on remote sensing: From AVHRR to EOS-MODIS, *Rem. Sens. Environ.*, **55**, 65-79, 1995.
12. Martonchik, J.V. Determination of aerosol optical depth and land surface directional reflectances using multiangle imagery, *J.Geophys.Res.*, **102**, 17015-17022, 1997.
13. Herman, M., J.L. Deuze, C. Devaux, P. Goloub, F-M Breon and D. Tanre, Remote sensing of aerosol over land surfaces including polarization measurements and application to POLDER measurements, *J.Geophys.Res.*, **102**, 17039-17049, 1997.
14. T. Nakajima et al., Aerosol optical characteristics in the yellow sand events observed in May, 1982 at Nagasaki - Part II Models, *J. Meteorol. Soc. Japan*, **67**, 279-291, 1989.
15. M.I. Mishchenko, Light scattering by size-shape distributions of randomly oriented axially symmetric particles of a size comparable to a wavelength, *Appl. Opt.*, **32**, 4652-4666, 1993.
16. Russell, E.E., F.G. Brown, R.A. Chandos, W.C. Fincher, L.F. Kubel, A.A. Lacis, and L.D. Travis, Galileo Photopolarimeter/Radiometer experiment, *Space Sci. Rev.*, **60**, 531-563 (1992).
17. Cairns, B, B.E. Carlson, A.A. Lacis and E. Russell, Analysis of ground-based polarimetric sky radiance measurements, *Proc. SPIE*, **3121**, 1997.
18. Rondeaux, G. and M. Herman, Polarization of light reflected by crop canopies, *Remote Sens. Environ.*, **38**, 63-75, 1991.
19. Vanderbilt, V.C., L. Grant, L..L. Biehl and B.F. Robinson, Specular, diffuse and polarized light scattered by two wheat canopies, *Appl.Opt.*, **24**, 2408-2418, 1985.
20. Breon, F-M, D. Tanre, P. Lecomte and M. Herman, Polarized reflectance of bare soils and vegetation: Measurements and models, *IEEE Trans. Geo. Rem. Sens*, **33**, 487-499, 1995.
21. J.F. de Haan, P.B. Bosma and J.W. Hovenier, The adding method for multiple scattering calculations of polarized light. *Astronom.Astrophys.*, **183**, 371, 1987.
22. Born, M and E. Wolf, *Principles of Optics*, Pergamon Press, Oxford 1980.
23. Saunders, P.M., Shadowing on the ocean and the existence of the horizon, *J.Geophys.Res.*, **72**, 4643-4649, 1967.